Int. J. Heat Mass Transfer. Vol. 17, pp. 223–240. Pergamon Press 1974. Printed in Great Britain

ON MERK'S METHOD OF CALCULATING BOUNDARY LAYER TRANSFER

B. T. CHAO
Department of Mechanical Engineering, University of Illinois at Urbana-Champaign, Urbana. Illinois 61801, U.S.A.

and

R. O. FAGBENLE
Mechanical Engineering Department, University of Science and Technology, Kumasi, Ghana.

(*Received* 25 *July* 1973)

Abstract—Merk's procedure for the computation of boundary layer transfer using wedge solutions is examined in detail. The differential equations governing the universal function in the second term of his series solution for the momentum and the energy boundary layer equation are in error. Numerical solutions for the corrected equations have been obtained. In addition, the universal functions associated with the two higher order terms are evaluated and tabulated. With the availability of such information, an assessment of the accuracy of the results can be made. Examples illustrating the usefulness as well as limitations of the method are given.

NOMENCLATURE

c_f, skin friction coefficient defined in (28);
D, diameter of circular cylinder;
h, local heat transfer coefficient;
k, thermal conductivity;
L, reference length;
Nu, Nusselt number defined in (33);
Pr, Prandtl number;
r, radial distance from a surface element to the axis of a rotationally symmetrical body;
Re, Reynolds number, appropriately defined where used;
T, temperature;
u, velocity component in x-direction;
U, velocity at outer edge of boundary layer;
v, velocity component in y-direction;
x, streamwise coordinate measured along surface from front stagnation point;
y, coordinate normal to surface;
α, thermal diffusivity;
η, dimensionless coordinate defined in (7);
Λ, wedge variable defined in (10);
μ, dynamic viscosity;
ξ, dimensionless coordinate defined in (7);
ν, kinematic viscosity;
ρ, mass density;
τ_w, shear stress at wall.

Subscripts

w, wall condition;
∞, free stream condition.

Other symbols are defined in the text.

1. INTRODUCTION

THE NEED for a general yet simple procedure for predicting the transport behaviour of boundary-layer flows has long been recognized. Blasius [1] was among the first to introduce the use of universal functions in the solution of steady, two-dimensional, laminar, constant property boundary layer equations. The method requires that the external stream velocities be expressed as polynomials of the streamwise distance measured from the front stagnation point. Generally speaking, the Blasius series is quite effective for flows over blunt objects. In the case of slender bodies, an excessive number of terms would be required in the polynomial representation and the series suffers from slow convergence. In an attempt to remedy this drawback, Görtler [2] devised another series solution based on the momentum equation in stretched coordinates which are essentially those defined in equation (7). The solution was also expressed in terms of universal functions. The convergence of Görtler's series is not always superior to that of Blasius as has been demonstrated by Frössling [3]. Görtler's method was employed by Sparrow [4] for the analysis of thermal boundary layers. It was found that considerably more universal functions were required and, as one might expect, Sparrow's procedure shared the shortcomings of Görtler's method.

A procedure which belongs to the category of 'wedge' methods and which provides a rigorous refinement of the local similarity concept is that of Merk [5]. Following Görtler and Meksyn [6], Merk

derived the momentum and energy boundary layer equations in the transformed, coordinates (ξ, η). In common with Görtler's method, his series solution is also expressed in terms of universal functions. The point of departure is that Görtler expanded the 'wedge' variable Λ in series of ξ while Merk chose the inverse expansion and adopted Λ as one of the independent coordinates. Merk evaluated the first term in the series by the asymptotic integration method propounded by Meksyn. As in Görtler's series, the first term corresponds to the local similarity solution. Merk presented the differential equation for the second term but gave no solution. While we speak of Merk's method, it is appropriate to mention, as was done in his paper, that the method is an extension or refinement of Meksyn's procedure.

Spalding and Pun [7] reviewed fifteen methods for predicting laminar heat transfer coefficients at the surface of an isothermal object. Each method was applied to the calculation of local Nusselt number over the front portion of a circular cylinder in cross-flow. The results were compared with the solution of Frössling [8] and the experimental data of Schmidt and Wenner [9]. Frössling's solution was regarded as 'exact' for $0 \leqslant x/D \leqslant 0{\cdot}45$. On the basis of this study, Merk's method was rated among the top five for its accuracy. However, it should be noted that only the first term of the series was available then. Spalding and Pun also cautioned that their results could not be taken as generally valid. Had a surface other than the leading portion of a circular cylinder been chosen and a streamlined object used instead, the conclusion might have been different.

Evans [10] numerically integrated the differential equation governing the second term in Merk's series for both the flow and the temperature boundary layer equation. Based on the several examples studied, Evans recorded the unexpected finding: "Indeed, there is some evidence, but this is not conclusive, that the use of just one term in the series will generally give better agreement with the other methods and with experiment than the use of two terms, . . . " A re-examination of the form of the series solution appropriate to the governing equations led the first author (BTC) to discover that the differential equations given by Merk for the second term of the series for both the flow and the temperature boundary layer were in error. So were the equations used by Evans. This is particularly unfortunate in view of the fact that Evans performed extensive numerical computations based on the incorrect equations. The error in Merk's equation was earlier reported by Bush [11] in a brief research note which apparently escaped Evans' attention. Nor were we aware of the work until the final stage of this investigation. However, the "corrected" equation presented by Bush contains not only the wedge variable but also a second parameter involving its derivatives, namely,

$$\xi \frac{\mathrm{d}^2\Lambda}{\mathrm{d}\xi^2} \Big/ \frac{\mathrm{d}\Lambda}{\mathrm{d}\xi}.$$

An essential feature of Merk's scheme is that it makes possible rapid calculations of the significant boundary layer quantities with the aid of a limited number of universal functions which can be tabulated once and for all. This advantage is to a large extent lost if Bush's development is followed.

The purpose of the present investigation is to present a reappraisal of Merk's procedure by providing, first, the corrected sequence of the differential equations governing the universal functions associated with the method and, secondly, to provide a tabulation of these and other related functions. With the availability of such tabulation, the determination of the local wall shear and the surface heat transfer rates over smooth, isothermal objects of arbitrary shape becomes a simple matter, once the outer stream velocity distribution is known. The development of the boundary layer and details of the velocity and temperature fields can be obtained with equal ease.

2. GOVERNING EQUATIONS

The conservation equations for steady, laminar, non-dissipative, constant property, two-dimensional or rotationally symmetrical boundary layer flows are well known and are given in Merk's paper. For the convenience of the reader, they are reproduced below.

$$\left(u\frac{\partial}{\partial x} + v\frac{\partial}{\partial y}\right)u = U\frac{\mathrm{d}U}{\mathrm{d}x} + \nu\frac{\partial^2 u}{\partial y^2}, \tag{1}$$

$$\frac{\partial(ru)}{\partial x} + \frac{\partial(rv)}{\partial y} = 0, \tag{2}$$

$$\left(u\frac{\partial}{\partial x} + v\frac{\partial}{\partial y}\right)T = \alpha\frac{\partial^2 T}{\partial y^2}. \tag{3}$$

In the continuity equation, r is the radial distance from a surface element to the axis of the rotationally symmetrical body. It should be dropped for two-dimensional flows.

The boundary conditions considered by Merk are,

$$\text{for} \quad y = 0 : u = v = 0 \quad \text{and} \quad T = T_w \tag{4}$$

$$\text{for} \quad y \to \infty : u = U(x) \quad \text{and} \quad T = T_\infty. \tag{5}$$

Both T_w and T_∞ are constants.

The continuity equation is identically satisfied by introducing a stream function $\psi(x, y)$ defined by

$$u = \frac{L}{r}\frac{\partial \psi}{\partial y}, \qquad v = -\frac{L}{r}\frac{\partial \psi}{\partial x}. \tag{6}$$

In (6) and other equations which follow, one needs only to set $r = L$ for two-dimensional flows. The (x, y) coordinate system is transformed into the dimensionless (ξ, η) system according to,

$$\xi = \int_0^x \frac{U}{U_\infty}\frac{r^2}{L^2}\frac{\mathrm{d}x}{L}, \qquad \eta = \left(\frac{Re}{2\xi}\right)^{\frac{1}{2}}\frac{U}{U_\infty}\frac{r}{L}\frac{y}{L}, \tag{7}$$

where U_∞ is a reference velocity, taken as the undisturbed, uniform velocity of the oncoming flow and $Re = U_\infty L/\nu$. A dimensionless stream function f is introduced, such that

$$\psi(x, y) = U_\infty L(2\xi/Re)^{\frac{1}{2}} f(\xi, \eta). \tag{8}$$

It follows then

$$\frac{u}{U} = \frac{\partial f}{\partial \eta}, \tag{9a}$$

$$-\frac{v}{U}(2\xi Re)^{\frac{1}{2}}\frac{L}{r} = f + 2\xi\frac{\partial f}{\partial \xi} + \left(\Lambda + \frac{2\xi}{r}\frac{\mathrm{d}r}{\mathrm{d}\xi} - 1\right)\eta\frac{\partial f}{\partial \eta}, \tag{9b}$$†

where Λ is the 'wedge variable' defined by

$$\Lambda = \frac{2\xi}{U}\frac{\mathrm{d}U}{\mathrm{d}\xi}. \tag{10}$$

It was named by Görtler as the principal function. The outcome of the transformation is that the momentum equation becomes

$$f''' + ff'' + \Lambda[1 - (f')^2] = 2\xi\frac{\partial(f', f)}{\partial(\xi, \eta)}, \tag{11}$$

and the boundary conditions are

$$f = f' = 0 \quad \text{for} \quad \eta = 0, \quad \text{and} \quad f' = 1 \quad \text{for} \quad \eta \to \infty. \tag{12}$$‡

The primes denote differentiation with respect to η while $\partial(f', f)/\partial(\xi, \eta)$ is the Jacobian. Upon introducing a dimensionless temperature function θ defined by

$$\frac{T - T_w}{T_\infty - T_w} = \theta(\xi, \eta), \tag{13}$$

the thermal energy equation transforms to

$$\theta'' + Pr f\theta' = 2Pr\xi\frac{\partial(\theta, f)}{\partial(\xi, \eta)}. \tag{14}$$

The boundary conditions are

$$\theta = 0 \quad \text{for} \quad \eta = 0, \quad \text{and} \quad \theta = 1 \quad \text{for} \quad \eta \to \infty. \tag{15}$$

At this juncture, Merk made a pivotal step in his development. Since Λ depends only on x, so does ξ. Hence, one may regard Λ as a function of ξ, as was the view taken by Görtler, or, conversely, one may regard ξ as a function of Λ. On this basis, Merk wrote the solution of (11) as follows,

$$f(\xi, \eta) = f_0(\Lambda, \eta) + 2\xi\frac{\mathrm{d}\Lambda}{\mathrm{d}\xi}f_1(\Lambda, \eta) + \ldots. \tag{16}$$

Substituting (16) into (11) and (12), followed by equating coefficients, he found

$$\left.\begin{aligned} &f_0''' + f_0 f_0'' + \Lambda[1 - (f_0')^2] = 0 \\ &\text{with} \\ &f_0 = f_0' = 0 \quad \text{for} \quad \eta = 0, \quad \text{and} \quad f_0' = 1 \\ &\qquad\qquad \text{for} \quad \eta \to \infty. \end{aligned}\right\} \tag{17}$$

However, the equation for f_1 given by Merk was incorrect. Because of the presence of the Jacobian in (11), the differential equation for f_1 depends on how one chooses to express the third term in (16). If one treats $2\xi(\mathrm{d}\Lambda/\mathrm{d}\xi)$ as a small expansion parameter and writes the third term as

$$\frac{1}{2}\left(2\xi\frac{\mathrm{d}\Lambda}{\mathrm{d}\xi}\right)^2 f_2(\Lambda, \eta),$$

as was done by Bush, then

$$\left.\begin{aligned} &f_1''' + f_0 f_1'' - 2\Lambda f_0' f_1' + f_0'' f_1 \\ &\quad + 2\left(1 + \xi\frac{\mathrm{d}^2\Lambda}{\mathrm{d}\xi^2}\Big/\frac{\mathrm{d}\Lambda}{\mathrm{d}\xi}\right)(f_0'' f_1 - f_0' f_1') \\ &\qquad\qquad = \frac{\partial(f_0', f_0)}{\partial(\Lambda, \eta)} \\ &\text{with} \\ &f_1 = f_1' = 0 \quad \text{for} \quad \eta = 0, \quad \text{and} \quad f_1' = 0 \\ &\qquad\qquad \text{for} \quad \eta \to \infty. \end{aligned}\right\} \tag{18}$$

† In equation (11b) of Merk's paper, the term $2\xi/r\ \mathrm{d}r/\mathrm{d}\xi$ is inadvertently omitted.

‡ In general, the first boundary condition should read $f + 2\xi(\partial f/\partial\xi) = 0$ as is obvious from equation (9b). However, for impervious surface, it is possible to assign $f = 0$ at the wall and hence $\partial f/\partial\xi$ also vanishes.

When one compares (18) with the corresponding equation given by Merk, one finds that the term involving $2[1 + \xi(d^2\Lambda/d\xi^2)/(d\Lambda/d\xi)]$ is missing. The solution of (18) would obviously depend on Λ and $\xi[(d^2\Lambda/d\xi^2)/(d\Lambda/d\xi)]$. Hence, it is totally impractical for tabulatiion. This difficulty is overcome by choosing a different series for $f(\xi, \eta)$. Accordingly, we write

$$f(\xi,\eta) = f_0(\Lambda,\eta) + 2\xi\frac{d\Lambda}{d\xi}f_1(\Lambda,\eta) + 4\xi^2\frac{d2\Lambda}{d\xi^2}f_2(\Lambda,\eta) + \left(2\xi\frac{d\Lambda}{d\xi}\right)^2 f_3(\Lambda,\eta) + \left(2\xi\frac{d\Lambda}{d\xi}\right)\left(4\xi^2\frac{d^2\Lambda}{d\xi^2}\right)f_{1,2}(\Lambda,\eta) + \ldots. \quad (19)$$

Upon substituting (19) into (11) and (12) and equating coefficients, we find that the equation for f_0 remains unaltered, but the equation for f_1 becomes

$$\left.\begin{aligned} &f_1''' + f_0 f_1'' - 2(1+\Lambda)f_0' f_1' + 3f_0'' f_1 = \\ &\qquad = \frac{\partial(f_0', f_0)}{\partial(\Lambda,\eta)}, \\ &\text{with} \\ &f_1 = f_1' = 0 \quad \text{for} \quad \eta = 0, \quad \text{and} \quad f_1' = 0 \\ &\qquad \text{for} \quad \eta \to \infty. \end{aligned}\right\} \quad (20)$$

The remaining two equations in the hierarchy for which numerical solutions have been obtained are:

$$\left.\begin{aligned} &f_2''' + f_0 f_2'' - 2(2+\Lambda)f_0' f_2' + 5f_0'' f_2 = f_0' f_1' \\ &\qquad - f_0'' f_1, \\ &\text{with} \\ &f_2 = f_2' = 0 \quad \text{for} \quad \eta = 0, \quad \text{and} \quad f_2' = 0 \\ &\qquad \text{for} \quad \eta \to \infty, \end{aligned}\right\} \quad (21)$$

and

$$\left.\begin{aligned} &f_3''' + f_0 f_3'' - 2(2+\Lambda)f_0' f_3' + 5f_0'' f_3 \\ &\quad = \frac{\partial(f_1', f_0)}{\partial(\Lambda,\eta)} + \frac{\partial(f_0', f_1)}{\partial(\Lambda,\eta)} + (2+\Lambda)(f_1')^2 \\ &\qquad - 3f_1 f_1'' \\ &\text{with} \\ &f_3 = f_3' = 0 \quad \text{for} \quad \eta = 0, \quad \text{and} \quad f_3' = 0 \\ &\qquad \text{for} \quad \eta \to \infty. \end{aligned}\right\} \quad (22)$$

An inspection of the foregoing set of equations shows that they can be integrated as if they were ordinary differential equations since, for any given streamwise location, Λ is fixed. Furthermore, all f_i's $(i = 0, 1, 2, \ldots)$ are universal in the sense that they depend on a single parameter Λ. As such, they can be tabulated once and for all.

The appropriate series solution for (14) is analogous to that for (11). It is

$$\theta(\xi,\eta) = \theta_0(\Lambda,\eta) + 2\xi\frac{d\Lambda}{d\xi}\theta_1(\Lambda,\eta) + 4\xi^2\frac{d^2\Lambda}{d\xi^2}\theta_2(\Lambda,\eta) + \left(2\xi\frac{d\Lambda}{3\xi}\right)^2\theta_3(\Lambda,\eta) + \left(2\xi\frac{d\Lambda}{d\xi}\right)\left(4\xi^2\frac{d^2\Lambda}{d\xi^2}\right)\theta_{1,2}(\Lambda,\eta) + \ldots \quad (23)$$

A straight forward calculation leads to the following set:

$$\left.\begin{aligned} &Pr^{-1}\theta_0'' + f_0\theta_0' = 0, \\ &\text{with} \\ &\theta_0 = 0 \quad \text{for} \quad \eta = 0, \theta_0 = 1 \quad \text{for} \quad \eta \to \infty, \end{aligned}\right\} \quad (24)$$

$$Pr^{-1}\theta_1'' + f_0\theta_1' - 2f_0'\theta_1 = \frac{\partial(\theta_0, f_0)}{\partial(\Lambda,\eta)} - 3f_1\theta_0', \quad (25)$$

$$Pr^{-1}\theta_2'' + f_0\theta_2' - 4f_0'\theta_2 = f_0'\theta_1 - f_1\theta_0' - 5f_2\theta_0', \quad (26)$$

$$Pr^{-1}\theta_3'' + f_0\theta_3' - 4f_0'\theta_3 = \frac{\partial(\theta_1, f_0)}{\partial(\Lambda,\eta)} + \frac{\partial(\theta_0, f_1)}{\partial(\Lambda,\eta)} + 2f_1'\theta_1 - 3f_1\theta_1' - 5f_3\theta_0', \quad (27)$$

etc. The boundary conditions for the last three equations are: $\theta_i = 0$ for $\eta = 0$ and for $\eta \to \infty$, where $i = 1, 2$ or 3.

3. FRICTION COEFFICIENT, DISPLACEMENT AND MOMENTUM THICKNESS, AND NUSSELT NUMBER

The equations for f_i and $\theta_i (i = 0, 1, 2$ and $3)$ have been numerically integrated and the main results are tabulated in the Appendix. With the aid of such tabulation, the calculation of local wall shear, the development of the displacement and momentum thickness and the local Nusselt number become a simple matter. The necessary input is the streamwise velocity distribution at the edge of the boundary layer, $U(x)$, which may be deduced from experiments or estimated from theory. In this section, we have brought together the various formulas required for the calculation.

Defining the local friction coefficient by

$$c_f = \frac{\mu(\partial u/\partial y)_{y=0}}{\frac{1}{2}\rho U_\infty^2}, \quad (28)$$

we find, after transformation,

$$\tfrac{1}{2}c_f Re^{\frac{1}{2}} = \frac{r}{L}\left(\frac{U}{U_\infty}\right)^2 (2\xi)^{-\frac{1}{2}}\left[f_0''(\Lambda,0) + 2\xi\frac{d\Lambda}{d\xi}f_1''(\Lambda,0) + 4\xi^2\frac{d^2\Lambda}{d\xi^2}f_2''(\Lambda,0) + \left(2\xi\frac{d\Lambda}{d\xi}\right)^2 f_3''(\Lambda,0) + \ldots\right] \tag{29}$$

in which $Re = U_\infty L/\nu$, as has previously been defined.

The displacement and the momentum thickness are defined in the usual way, i.e.

$$\delta_1 = \int_0^\infty \left(1 - \frac{u}{U}\right)dy \quad \text{and} \quad \delta_2 = \int_0^\infty \frac{u}{U}\left(1 - \frac{u}{U}\right)dy, \tag{30}$$

and the corresponding dimensionless counterparts are

$$\delta_1^* = \int_0^\infty (1 - f')\,d\eta = \frac{r}{L}\frac{U}{U_\infty}\left(\frac{Re}{2\xi}\right)^{\frac{1}{2}}\frac{\delta_1}{L}, \tag{31a}$$

$$\delta_2^* = \int_0^\infty f'(1 - f')\,d\eta = \frac{r}{L}\frac{U}{U_\infty}\left(\frac{Re}{2\xi}\right)^{\frac{1}{2}}\frac{\delta_2}{L}. \tag{31b}$$

It can be demonstrated that,

$$\delta_1^* = \delta_{1,s}^* - 2\xi\frac{d\Lambda}{d\xi}f_1(\Lambda,\infty) - 4\xi^2\frac{d^2\Lambda}{d\xi^2}f_2(\Lambda,\infty) - \left(2\xi\frac{d\Lambda}{d\xi}\right)^2 f_3(\Lambda,\infty) - \ldots, \tag{32a}$$

where

$$\delta_{1,s}^* = [\eta - f_0(\Lambda,\eta)]_{\eta\to\infty},$$

and

$$\delta_2^* = \delta_{2,s}^* + 2\xi\frac{d\Lambda}{d\xi}I_1 + 4\xi^2\frac{d^2\Lambda}{d\xi^2}I_2 + \left(2\xi\frac{d\Lambda}{d\xi}\right)^2 I_3 + \ldots \tag{32b}$$

where

$$\delta_{2,s}^* = \int_0^\infty f_0'(1 - f_0')\,d\eta, \qquad I_1 = \int_0^\infty f_1'(1 - 2f_0')\,d\eta,$$

$$I_2 = \int_0^\infty f_2'(1 - 2f_0')\,d\eta,$$

$$\text{and} \quad I_3 = \int_0^\infty [f_3'(1 - 2f_0') - (f_1')^2]\,d\eta.$$

We note that $\delta_{1,s}^*$ and $\delta_{2,s}^*$ are respectively the displacement and momentum thickness associated with the locally similar boundary layer. These boundary layer functions are also tabulated in the Appendix.

We define the local Nusselt number as

$$Nu = \frac{hL}{k} = -\frac{L(\partial T/\partial y)_{y=0}}{T_w - T_\infty} = L\left(\frac{\partial\theta}{\partial y}\right)_{y=0}, \tag{33}$$

as was done by Merk. It follows then

$$NuRe^{-\frac{1}{2}} = \frac{r}{L}\frac{U}{U_\infty}(2\xi)^{-\frac{1}{2}}\left[\theta_0'(\Lambda,0) + 2\xi\frac{d\Lambda}{d\xi}\theta_1'(\Lambda,0) + 4\xi^2\frac{d^2\Lambda}{d\xi^2}\theta_2'(\Lambda,0) + \left(2\xi\frac{d\Lambda}{d\xi}\right)^2\theta_3'(\Lambda,0) + \ldots\right]. \tag{34}$$

4. NUMERICAL SOLUTIONS AND ESTIMATES OF THEIR ACCURACY

The differential equations for f_i and $\theta_i (i = 0, 1, 2$ and 3) given in Section 2 were numerically integrated using a seven-term Taylor expansion scheme on IBM 360/75 digital computing system. The double precision arithmetic was employed in all computations. Data for twenty-seven values of Λ ranging from $-0{\cdot}15$ to $1{\cdot}0$ and for seven values of Pr ranging from $0{\cdot}01$ to 100 have been computed and tabulated. A few cursory comments on our experience are given below; details may be found in a dissertation by Fagbenle [12].

Very high accuracy is required of the basic function f_0 since the higher order functions in the hierarchy are sensitive to its variation. The selection of the integration step size depends on the precision of the numerical results desired, the number of terms retained in the Taylor expansion, the iterative scheme used, and the computation time allowed. After several trials, the integration step sizes finally selected were: $\Delta\eta = 0{\cdot}005$ for $0 < \eta < 0{\cdot}1$ and $\Delta\eta = 0{\cdot}01$ for $\eta \geqslant 0{\cdot}1$. The iteration was to continue until the following condition was met:

$$|1 - f_0'(\Lambda,\eta_\infty)| < 10^{-12}$$

where η_∞ denotes some large value of η. A value of 8 was found to be adequate in that the computed second wall derivative $f_0''(\Lambda,0)$ exhibited no change up to the twelfth significant digit when the computation was repeated with $\eta_\infty > 8$. The results for $f_0''(\Lambda,0)$ obtained in this way agreed with those published by Elzy and Sisson [13] within very close limits for all Λ's investigated. For example, when $\Lambda = -0{\cdot}19$, we find $f_0''(\Lambda,0) = 0{\cdot}08569975180$ which may be compared with $0{\cdot}085699745$ reported by Elzy

and Sisson. When $\Lambda = 1{\cdot}0$, the corresponding values are 1·23258765687 and 1·2325877.

The integration of the f_1 equation requires the evaluation of the derivatives $\partial f_0/\partial\Lambda$ and $\partial f_0'/\partial\Lambda$. A second order central difference representation was used, i.e.

$$\frac{\partial f_0}{\partial\Lambda} \simeq \frac{-f_0(\Lambda + 2\Delta\Lambda, \eta) + 8f_0(\Lambda + \Delta\Lambda, \eta) - 8f_0(\Lambda - \Delta\Lambda, \eta) + f_0(\Lambda - 2\Delta\Lambda, \eta)}{12\Delta\Lambda}$$

and the final choice of $\Delta\Lambda$ was 0·001. The integration step sizes used for f_1 and f_2 were the same as those used for f_0 but larger values were used for f_3 as the demand on accuracy became less stringent. A more relaxed condition

$$|f_i'(\Lambda, \eta_\infty)| < 10^{-6}, i = 1, 2, 3$$

was used to halt iteration in order to conserve computation time. Unlike the case of f_0, further iteration beyond this point did not produce significant reduction in the residue $|f_i'(\Lambda, \eta_\infty)|$ and only very minor change in $f_i''(\Lambda, 0)$ was observed.

We are not aware of any direct means of ascertaining the accuracy of our numerical program for f_1. A possible approach is to select flow situations for which solutions are available and for which the contribution of f_1 is greater than that of f_2 and f_3 by an order of magnitude. It has been found that at suitable locality in the linearly retarded stream of Howarth [14] and of the forward portion of a circular cylinder in crossflow, the calculation of the local skin friction coefficient satisfies the foregoing requirement. In Table 1(a), the results for the Howarth flow are compared with those reported by Hartree [15] and by Schönauer [16] in addition to those given by Howarth himself. Schönauer employed a finite difference scheme in which h denotes the mesh size in the direction of the main stream and n is the number of subdivisions normal to it. In Table 1(b) the data for a circular cylinder in cross flow are compared with the difference-differential solutions of Terrill [17] and the finite difference solutions of Schönauer. The evidence presented, though limited in scope, lends support to our contention that the numerical program is satisfactory.

Very high accuracy is also required of the temperature function θ_0 for the same reason as that given for f_0. As one might expect, the Prandtl number has a decisive influence on η_∞: when $Pr = 100$, $\eta_\infty \simeq 1{\cdot}8$ and when $Pr = 0{\cdot}01$, $\eta_\infty \simeq 60$. The integration step sizes used were identical to those selected for f_0 when $Pr \geqslant 0{\cdot}7$. However, for $Pr = 0{\cdot}1$ and $0{\cdot}01$, $\Delta\eta$ was increased to 0·05 for $\eta \geqslant 5$. The wall derivatives $\theta_0'(\Lambda, 0)$ evaluated in this manner agree with the data reported by Elzy and Sisson up to the eighth (which is also the last) significant digit for the entire range of Pr and Λ investigated.

A second order central difference scheme was used for the evaluation of $\partial\theta_0/\partial\Lambda$ and $\partial\theta_1/\partial\Lambda$, as was done for the computation of $\partial f_0/\partial\Lambda$. For all Pr greater than 0·1, $\Delta\Lambda$ was also 0·001. However, in the case of $Pr = 0{\cdot}1$ and $0{\cdot}01$, the computed results for θ_3 were not satisfactory when Λ is close to unity. In this region, θ_1 becomes relatively insensitive to changes in Λ. There is some evidence that the roundoff errors might be accentuated as extended regions of integra-

Table 1. Comparison of $\frac{1}{2}c_f Re^{\frac{1}{2}}$ calculated from different methods

(a) Howarth flow, $U = U_\infty(1 - x/L)$, $\frac{1}{2}c_f = \tau_w/\rho U^2$, and $Re = Ux/\nu$

			Schönauer		Present study			
					No. of terms in equation (29)			
x/L	Howarth	Hartree	$n = 300$, $h = 5 \times 10^{-4}$	200, $2{\cdot}5 \times 10^{-4}$	1	2	3	4
0·0250	0·29102	0·29188	0·29130	0·29170	0·27924	0·29216	0·29171	0·29090

(b) Circular cylinder in cross flow, $U = 2U_\infty \sin 2x/D$, $\frac{1}{2}c_f = \tau_w/\rho U_\infty^2$, and $Re = U_\infty D/\nu$

		Schönauer		Present study			
				No. of terms in equation (29)			
$2x/D$	Terrill	$n = 300$, $h = 0{\cdot}005$	100, 0·005	1	2	3	4
0·30	1·4276	1·4276	1·4276	1·4263	1·4275	1·4275	1·4274
0·50	2·2300	2·2300	2·2304	2·2243	2·2302	2·2301	2·2300

tion are involved when the Prandtl number is small ($\eta_\infty \simeq 20$ for $Pr = 0{\cdot}1$ and $\eta_\infty \simeq 60$ for $Pr = 0{\cdot}01$). It is possible that improved results may be obtained by using a $\Delta\Lambda$ greater than 0·001, but this has not been done.

5. TABLES OF SIGNIFICANT WALL DERIVATIVES AND OTHER RELEVANT FUNCTIONS

In most applications, it is usually the surface characteristics, such as the local wall shear and the heat transfer rates, which are of interest. The calculation of these quantities requires only the information on the wall derivatives, as is obvious from (29) and (34). Those for the velocity functions $f_i''(\Lambda, 0)$ are given in Table A.1 in the Appendix and those for the temperature functions $\theta_i'(\Lambda, 0)$ are given in Table A.2(a)–(g) respectively for $Pr = 0{\cdot}01$, 0·1, 0·7, 1, 5, 10 and 100. One may notice that the data are tabulated at unequal intervals of Λ. The reasons are twofold. First, $\Lambda = 0{\cdot}5$ and 1 correspond respectively to the front stagnation point of the rotationally symmetrical and two-dimensional boundary layer flows. Second, in the vicinity of the front stagnation, either two-dimensional or rotationally symmetrical, Λ is a slowly varying function of ξ or x. Hence, in such regions, smaller increments in Λ are provided. The inaccuracies in the data are judged to be confined to the last digit quoted. For reasons already given some results for $Pr = 0{\cdot}1$ and 0·01 and for large values of Λ are uncertain and, hence, are omitted in the tabulation.

Table A.3 and Table A.4 are to be used in conjunction with (32a) and (32b) for the computation of the displacement and the momentum thickness of the boundary layer.

The determination of the velocity and the temperature fields in the boundary layer requires computer printouts of the f_i and θ_i functions. These are on deposit in the Heat Transfer Laboratory of the University of Illinois at Urbana-Champaign. Alternatively, they may be generated from the computer program developed in this study.

6. ILLUSTRATIONS

To evaluate the usefulness and limitations of Merk's method, a number of non-similar boundary layer flows have been analyzed. They include flows over inclined flat surfaces, flow over an airfoil, cross flows around elliptical cylinders of several aspect ratios including the circular cylinder and, for the rotationally symmetrical boundary layer, flow over a sphere. The local friction and heat transfer coefficients, the development of displacement and momentum thickness and the velocity and temperature fields are computed and compared with prior published results whenever possible. In the interest of conserving space, only a few are given here. Readers are referred to [12] for more complete information.

6.1 *Flow over inclined flat surface*

A well known boundary layer flow is that along a flat surface inclined at a small angle to the mainstream. The velocity at the edge of the boundary layer varies linearly with distance along the surface according to

$$\frac{U}{U_\infty} = 1 \pm \frac{x}{L} \tag{35}$$

where L is the inverse of the absolute magnitude of the velocity gradient $(\mathrm{d}/\mathrm{d}x)(U/U_\infty)$. In (35) and other expressions which follow, the positive sign is for accelerated flow and the negative is for decelerated flow. The case of the retarded flow was first studied in detail by Howarth. It is of particular interest since the reliability of most approximate methods deteriorates rapidly for boundary layers under an adverse pressure gradient even though they may be quite satisfactory for favourable pressure gradients. Furthermore, results of local friction coefficient evaluated by Schönauer [16] and by Smith and Clutter [18] who used a difference-differential scheme of integration are available for comparison.

If we write, for convenience, $C = 1 \pm (x/L)$, then $2\xi = \pm(C^2 - 1)$, $\Lambda = 1 - C^{-2}$, $2\xi(\mathrm{d}\Lambda/\mathrm{d}\xi) = 2C^{-2}(1 - C^{-2})$ and $4\xi^2(\mathrm{d}^2\Lambda/\mathrm{d}\xi^2) = -8C^{-2}(1 - C^{-2})^2$. The variations of these functions with distance measured along the surface are shown in Fig. 1. In retarded flows, $2\xi(\mathrm{d}\Lambda/\mathrm{d}\xi)$ is negative, but it is positive in accelerated flows and attains a maximum value of 0·5 at $x/L = 0{\cdot}4142$.

The computed wall friction data, expressed as $c_f Re^{\frac{1}{2}}/2$, ($c_f = 2\tau_w/\rho U^2$ and $Re = Ux/\nu$), are summarized in Table 2. In retarded flows, there is a significant difference between the present two-term results and those of Evans. The discrepancy is less pronounced in accelerated flows because the series in (29) is then dominated by the first term for which the equation given by Merk and later by Evans are identical to ours. It should be noted that the Merk series becomes semi-divergent for large negative values of Λ and, in such instance, Euler's transformation is employed for the evaluation of the sum. In Table 2, data calculated from the straight 4-term sum are also shown for the purpose of comparison. They are fenced in dotted rectangular boundaries. The series developed by Howarth was originally intended for retarded flows. As it turned out, it could be used for accelerated flows by simply changing the sign of

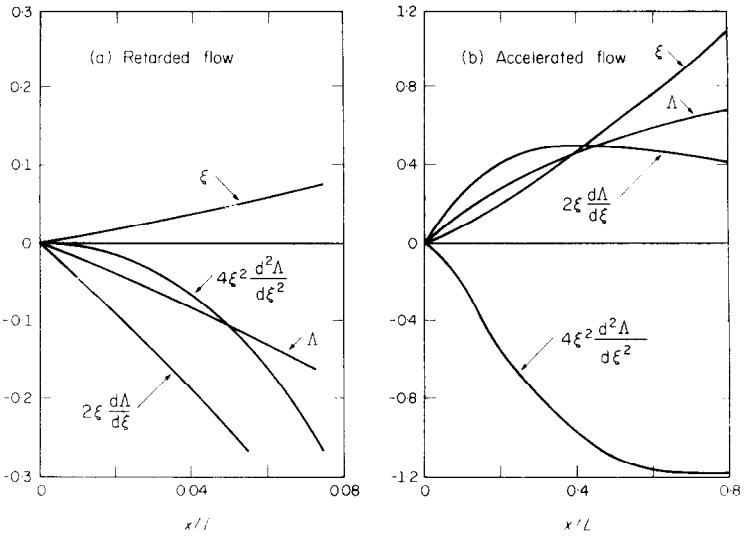

FIG. 1. Variation of ξ, Λ, $2\xi\ d\Lambda/d\xi$ and $4\xi^2\ d^2\Lambda/d\xi^2$ in linearly retarded and accelerated flows.

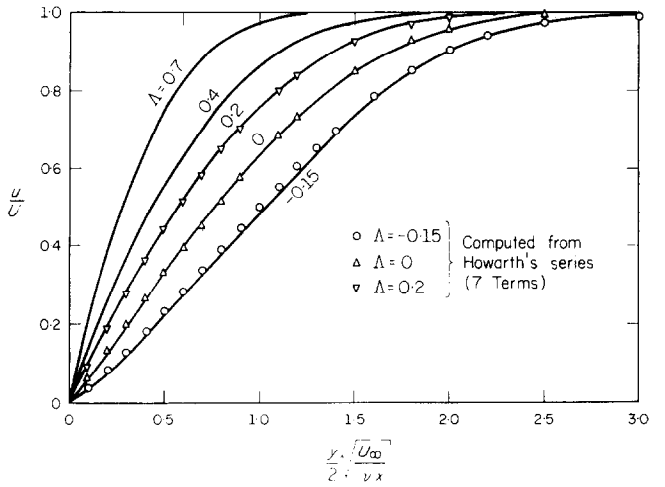

FIG. 2. Velocity distribution in boundary layers with linearly retarded and accelerated mainstream.

x/L in his series. However, it fails to converge for large values of x/L. When this occurs, the series is assumed to be semi-divergent† and Euler's method of finding the approximate sum is again used. The evidence provided by the data in Table 2 contradicts Evans' statement "Merk's approach, in common with many other general methods, appears to break down when it is applied to a retarded flow, certainly when it is used to estimate the drag coefficient, ... ".

We have also evaluated the u-velocity distribution using (9a) and (19). The results are shown as full lines in Fig. 2. Included for comparison are discrete data calculated from Howarth's series. The latter becomes unreliable for $\Lambda = 0{\cdot}4$ and $0{\cdot}7$, and hence, no comparison is made for these large Λ's.

The local heat transfer results, expressed as $NuRe^{-\frac{1}{2}}$ for an isothermal flat surface in a fluid of $Pr = 0{\cdot}7$ are summarized in Table 3. The data are, to a large extent, self-explanatory. The experimental information was reported by Büyüktür *et al.* [19]. While their study was aimed at examining the combined effects of free stream turbulence and pressure gradient on heat transfer, their measurements did include those for low levels of turbulence and for

† It is not certain if this assumption could be justified.

Table 2. Local friction coefficient, $\frac{1}{2}c_f Re^{\frac{1}{2}}$, for flow over an inclined flat surface
($c_f = \tau_w/\frac{1}{2}\rho U^2$, $Re = Ux/\nu$)

	x/L	A	Present results, no. of terms in series 1	2	3	4 Straight sum	4 Euler sum	Evans (1968) 2-term series	Howarth (1938), no. of terms in series 7	8	9 Straight sum	9 Euler sum	Smith and Clutter (1963)	Schönauer (1964)
Retarded flow	0·0675	−0·15	0·1503	0·2337	0·2260	0·1834	0·2070	0·3132	0·2065	0·2066	0·2063		0·205	0·206
	0·0465	−0·10	0·2231	0·2573	0·2553	0·2489	0·2512	0·2860	0·2511	0·2511	0·2510		0·251	0·252
	0·0241	−0·05	0·2813	0·2936	0·2933	0·2925		0·3030	0·2926	0·2926	0·2926		0·293	0·293
	0·0	0·0	0·3320	0·3320	0·3320	0·3320		0·3320	0·3321	0·3321	0·3321		0·321	
Accelerated flow	0·0541	0·10	0·4205	0·4083	0·4077	0·4070		0·4010	0·4067	0·4067	0·4067			
	0·1952	0·30	0·5717	0·5537	0·5513	0·5496		0·5451	0·5147	0·5901	0·4906	0·5460		
	0·4142	0·50	0·7100	0·6945	0·6915	0·6902		0·6884	(not useable)					
	0·8257	0·70	0·8519	0·8416	0·8391	0·8385		0·8382	(not useable)					

Table 3. Local heat transfer parameter, $NuRe^{-\frac{1}{2}}$, for flow over an inclined flat surface, $Pr = 0{\cdot}7$
($Nu = hL/k$, $Re = U_\infty L/\nu$)

	x/L	A	Present results, no. of terms in series 1	2	3	4 Straight sum	4 Euler sum	Evans (1968) 2-term series	Büyüktür *et al.* (1964), Mean of expt'l data	Büyüktür and Kestin (1965), no. of terms in series 5	6	7 Straight sum	7 Euler sum
Retarded flow	0·0675	−0·15	0·9408	0·9536	0·9547	0·9921	0·9491	0·9008		0·9615	0·9606	0·9602	
	0·0465	−0·10	1·2237	1·2249	1·2257	1·2319	1·2244	1·1928		1·2293	1·2291	1·2290	
	0·0241	−0·05	1·7989	1·7975*	1·7978	1·7989	1·7981	1·7793		1·7988	1·7988	1·7988	
	0·0541	0·10	1·3642	1·3681	1·3687	1·3695		1·3834		1·3699	1·3702	1·3701	
Accelerated flow	0·1048	0·1807	1·0400	1·0451	1·0463	1·0476		1·061	1·0357	1·0452	1·0519	1·0474	
	0·2009	0·3066	0·8223	0·8280	0·8300	0·8313		0·8440	0·8050	0·7797	0·9046	0·7427	0·8336
	0·4142	0·50	0·6654	0·6704	0·6730	0·6738		0·6808		−0·2267	3·0136	−5·6418	0·6778
	0·8257	0·70	0·5765	0·5798	0·5820	0·5824		0·5858		(not useable)			

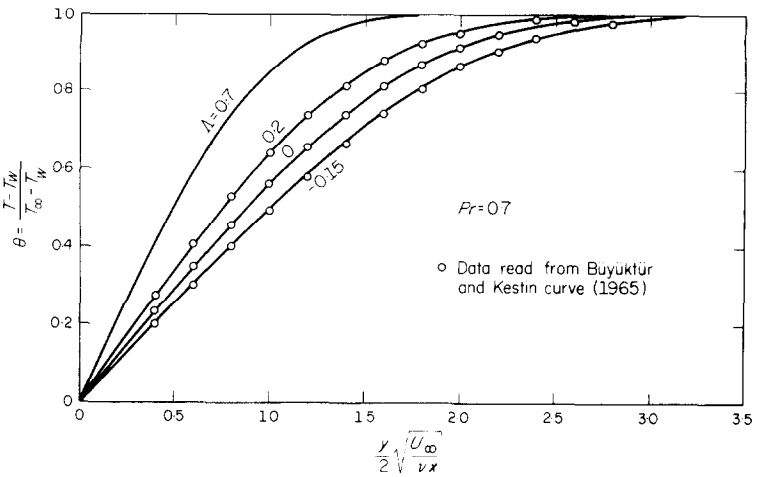

FIG. 3. Temperature distribution in boundary layers with linearly retarded and accelerated mainstream. $Pr = 0.7$.

laminar boundary layers. These were taken at $x/L = 0{\cdot}1048$ and $0{\cdot}2009$. Büyüktür and Kestin [20] obtained a series solution for the energy boundary layer equation using a method analogous to Howarth's. As such, it also fails to converge for large positive values of x/L In Fig. 3, the temperature profiles calculated from the 4-term Merk series for both retarded and accelerated flows are compared with data reported by Büyüktür and Kestin. The agreement is very good indeed. Temperature profiles for $Pr = 100$ have also been computed and they, too, exhibit excellent agreement.

6.2 *Elliptical cylinder in cross flow*

The Blasius–Frössling method of solution requires that the external stream velocity distribution be expressed in polynomials of x. For slender objects, such as an elliptical cylinder of large major-to-minor diameter ratio and oriented with its major axis parallel to the oncoming stream, the number of terms in the polynomial representation could become unwieldily large even if only modest accuracy is desired. This is a major handicap of the method as has long been known. The Merk method is free from this difficulty.

Schubauer [21] measured the velocity distribution in the two-dimensional laminar boundary layer over an elliptical cylinder using hot wire anemometry. The major and minor diameter of the cylinder were 11·78 and 3·98 inches respectively and, hence, the aspect ratio was 2·96. The impinging airstream was parallel to the major axis. Schubauer also measured the static pressure distribution along the surface and calculated therefrom U, dU/dx and d^2U/dx^2. He reported all data in appropriate dimensionless quantities, using the uniform velocity of the oncoming stream as the reference velocity and the minor diameter $2b$ of the ellipse as the reference length. If we denote: $\bar{U} = U/U_\infty$, and $\bar{x} = x/2b$, then

$$\left.\begin{aligned} \xi &= \int_0^{\bar{x}} \bar{U}\,d\bar{x},\ \Lambda = 2\xi\frac{\bar{U}'}{\bar{U}^2},\ \text{and} \\ \frac{d\Lambda}{d\xi} &= 2\frac{\bar{U}'}{\bar{U}^2} + 2\xi\frac{(\bar{U}')^2}{\bar{U}^4}\left[\frac{\bar{U}\bar{U}''}{(\bar{U}')^2} - 2\right], \end{aligned}\right\} \quad (36)$$

where the prime denotes differentiation with respect to $\bar{x}$. Schubauer tabulated the data for $\bar{U}$, $\bar{U}'$ and $\bar{U}\bar{U}''/(\bar{U}')^2$ at various $\bar{x}$'s and hence the Merk variables listed in (36) can be readily evaluated. The second derivative $(d^2\Lambda/d\xi^2)$ was computed from the first derivative using the central difference formula. The results so obtained are plotted in Fig. 4. In Schubauer's experiments, the first measurement station was located at $x/2b = 0{\cdot}175$. However, in the region $0 \leqslant x/2b \leqslant 0{\cdot}175$, the potential velocity distribution is expected to prevail. The dotted curves in Fig. 4 were based on the potential theory.

With the availability of information on Λ, $2\xi(d\Lambda/d\xi)$ and $4\xi^2(d^2\Lambda/d\xi^2)$, the u-component of the velocity field in the boundary layer can be easily computed with the aid of the computer printout for $f'_i(\Lambda, \eta)$. The results for $x/2b = 0{\cdot}545$, $1{\cdot}097$ and $1{\cdot}457$ are plotted and compared with Schubauer's measured data in Fig. 5. The agreement is as good as one may expect for the smallest $x/2b$ cited. The discrepancy is most pronounced for the largest $x/2b$ and in the outer region of the boundary layer. Once again, this is due to the fact that, under the said circumstance, the Merk series is non-converging and there are not

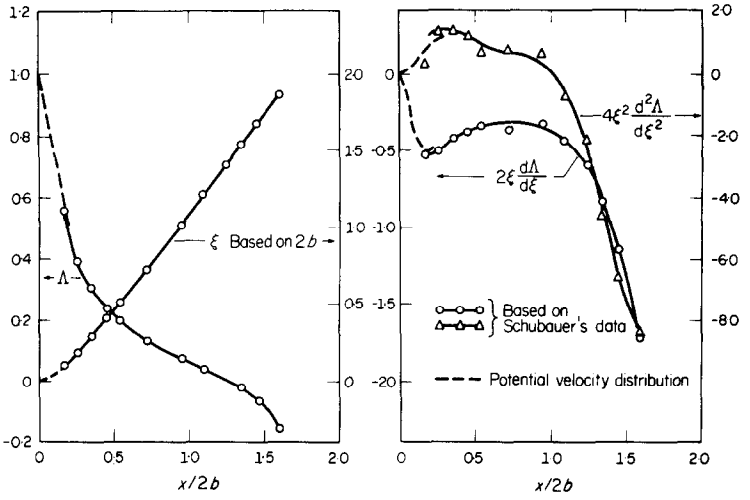

FIG. 4. Variation of ξ, Λ, $2\xi\ d\Lambda/d\xi$ and $4\xi^2\ d^2\Lambda/d\xi^2$ over Schubauer's elliptical cylinder. $a/b = 2{\cdot}96$.

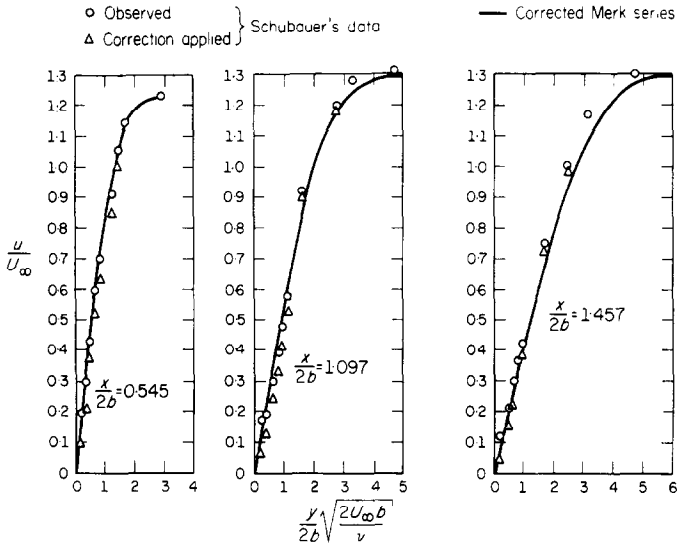

FIG. 5. Comparison of predicted velocity distribution in boundary layers over Schubauer's elliptical cylinder with experiments.

enough terms available for an effective application of Euler's procedure.

The local friction coefficient and the development of the displacement and the momentum thickness are displayed in Fig. 6. Portions of the curves are shown dotted because of the uncertainty in the sum of Merk's series. Included in the figure are the skin friction data reported by Smith and Clutter. In the region where the Merk series exhibits satisfactory convergence, the agreement is very good. The local heat transfer results evaluated from the 4-term Merk series for Pr ranging from 0·01 to 100 are exhibited in Fig. 7. We are not aware of any data available for comparison.

7. CONCLUDING REMARKS

Merk's method of analyzing the constant property, laminar boundary layer flows is theoretically sound and convenient to use. Since its introduction in 1959, it has not received the attention it deserves. This is probably due to the unfortunate error which Merk introduced into the differential equations governing

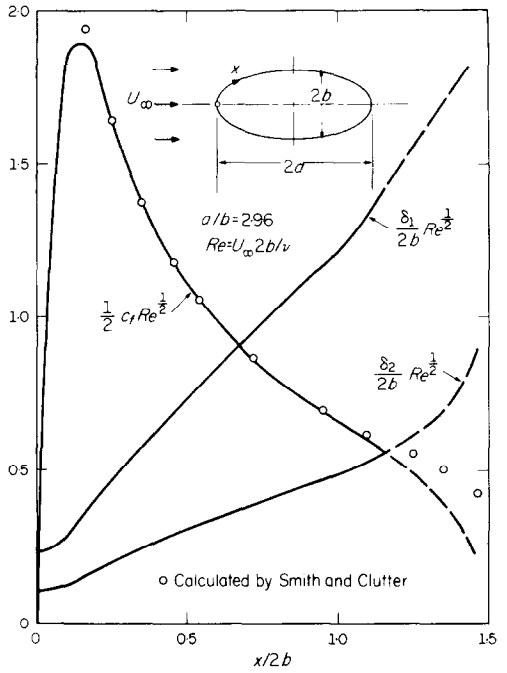

FIG. 6. Skin friction, displacement thickness and momentum thickness of boundary layer over Schubauer's elliptical cylinder.

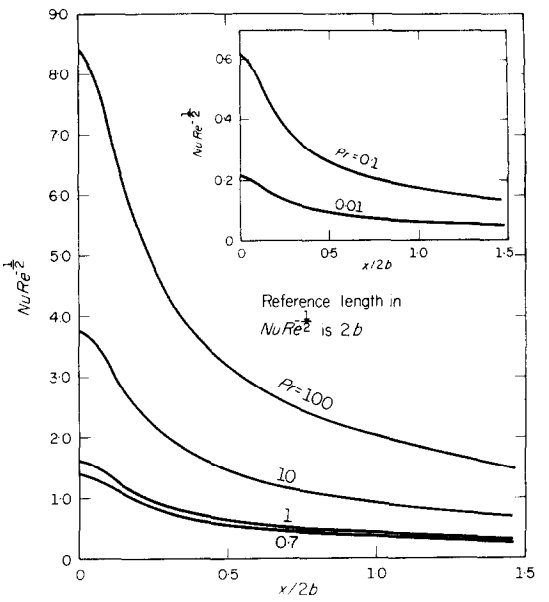

FIG. 7. Predicted variation of local Nusselt number over Schubauer's elliptical cylinder for various Prandtl numbers.

the universal functions. This error has led to misleading conclusions.

The appropriate series expansions for the flow function f and the temperature function θ are presented and the significant wall derivatives of the associated universal functions for the first four terms of the series solution have been tabulated for wide ranges of the wedge variable and of the fluid Prandtl number. With the aid of these tables, the local friction coefficient and the heat-transfer rates can be readily computed once the outerstream velocity distribution is known. The determination of the displacement and momentum thickness is likewise a simple matter. The nature of the convergence of the series provides an indication of the reliability of the results. Based on the large number of flow configurations examined in [12], including the two reported in this paper, it may be said that whenever the series exhibits rapid convergence, accurate results can be expected. There is some evidence, but it is not certain, that if the sum of the series (not necessarily convergent) is dominated by the first term, the result might still be expected to be satisfactory. When the series is semi-divergent, Euler's method of ascertaining the sum should be used. However, it is often not possible to obtain the accuracy one desires due to the limited number of terms available at the present time.

When the outer stream velocity distribution can be accurately described by polynomials of x with a limited number of terms, the Blasius series method of solution for the flow boundary layer and the Frössling series for the temperature boundary layer could yield results superior to Merk's, particularly for the region close to separation. This is the case for two-dimensional boundary layer flows over blunt bodies, such as a circular cylinder in cross flow. For slender objects, the excessively large number of terms required in the polynomial representation often precludes the use of the Blasius and the Frössling series. The Merk method is not subject to this limitation.

Acknowledgements—This work was partially supported by a National Science Foundation grant GK-16270. A major portion of the computer costs was borne by the Graduate College of the University of Illinois at Urbana-Champaign.

REFERENCES

1. H. Blasius, Grenzschichten in Flüssigkeiten mit kleiner Reibung, *Z. Math. Phys.* **56**, 1–37 (1908). English translation in NACA TM 1256.
2. H. Görtler, A new series for the calculation of steady laminar boundary layer flows, *J. Math. Mech.* **6**, 1–66 (1957).
3. N. Frössling, Problems of heat transfer across laminar boundary layers, *Theory and Fundamental Research in Heat Transfer*, edited by J. A. Clark. MacMillan (1963).
4. E. M. Sparrow, The thermal boundary layer on a non-isothermal surface with non-uniform free stream velocity. *J. Fluid Mech.* **4**, 321–329 (1958).

5. H. J. Merk, Rapid calculations for boundary-layer transfer using wedge solutions and asymptotic expansions, *J. Fluid Mech.* **5**, 460–480 (1959).
6. D. Meksyn, *New Methods in Laminar Boundary-Layer Theory*, Chapters 6, 7 and 9. Pergamon Press, Oxford (1961).
7. D. B. Spalding and W. M. Pun, A review of methods for predicting heat transfer coefficients for laminar uniform-property boundary layer flows, *Int. J. Heat Mass Transfer* **5**, 239–249 (1962).
8. N. Frössling, Evaporation, heat transfer, and velocity distribution in two-dimensional and rotationally symmetrical laminar boundary-layer flow, NACA TM 1432 (1958).
9. E. Schmidt and K. Wenner, Heat transfer on the circumference of a heated cylinder in transverse flow, NACA TM 1050 (1943).
10. H. L. Evans, *Laminar Boundary-Layer Theory*, Chapter 9. Addison-Wesley, Reading, Mass. (1968).
11. W. B. Bush, Local similarity expansions of the boundary-layer equations, *AIAA Jl* **2**, 1857–1858 (1964).
12. R. O. Fagbenle, On Merk's method of analyzing momentum, heat and mass transfer in laminar boundary layers, Ph.D. thesis, University of Illinois at Urbana-Champaign (1973).
13. E. Elzy and R. Sisson, Tables of similar solutions to the equations of momentum, heat and mass transfer in laminar boundary-layer flow, Bulletin No. 40, Engineering Experiment Station, Oregon State University, Corvallis, Oregon (1967).
14. L. Howarth, On the solution of the laminar boundary-layer equations, *Proc. R. Soc., Lond.* **164A**, 547–579 (1938).
15. D. R. Hartree, A solution of the laminar boundary-layer equation for retarded flow, British Report and Memorandum 2426 (1949).
16. W. Schönauer, Ein Differenzenverfahren zur Lösung der Grenzschichtgleichung fur stationare, laminare, inkompressible Strömung, *Ing.-Archiv.* **33**, 173–189 (1964).
17. R. M. Terrill, Laminar boundary-layer flow near separation with and without suction, *Phil. Trans. R. Soc., Lond.* **253Á** (1022), 55–100 (1960).
18. A. M. O. Smith and D. W. Clutter, Solution of the incompressible laminar boundary-layer equations, *AIAA Jl* **1**, 2062–2071 (1963).
19. A. R. Büyüktür, J. Kestin and P. F. Maeder, Influence of combined pressure gradient and turbulence on the transfer of heat from a plate, *Int. J. Heat Mass Transfer* **7**, 1175–1186 (1964).
20. A. R. Büyüktür and J. Kestin, Heat transfer across a linearly accelerated or decelerated laminar boundary layer, *J. Heat Transfer* **87C**, 403–408 (1965).
21. G. B. Schubauer, Air flow in a separating laminar boundary-layer, NACA TR 527 (1935).

APPENDIX

Table of Universal Functions in Merk's Method

Table A.1. Wall derivatives of velocity functions in Merk's series

Λ	$f''_0(\Lambda\,0)$		$f''_1(\Lambda,0)$		$f''_2(\Lambda,0)$		$f''_3(\Lambda,0)$	
−0·15	0·2163614060	00	−0·34791425	00	0·53071271	−01	−0·51628	00
−0·10	0·3192697599	00	−0·22259394	00	0·32254361	−01	−0·18908	00
−0·05	0·4003225954	00	−0·16658150	00	0·23117684	−01	−0·10318	00
0·0	0·4695999884	00	−0·13328326	00	0·17790554	−01	−0·65937	−01
0·05	0·5311296305	00	−0·11081394	00	0·14266708	−01	−0·45895	−01
0·10	0·5870352192	00	−0·94506819	−01	0·11760066	−01	−0·33722	−01
0·20	0·6867081810	00	−0·72319116	−01	0·84462348	−02	−0·20184	−01
0·25	0·7319408485	00	−0·64423273	−01	0·73029089	−02	−0·16183	−01
0·27	0·7493354864	00	−0·61675179	−01	0·69105119	−02	−0·14889	−01
0·30	0·7747545803	00	−0·57916482	−01	0·63789690	−02	−0·13203	−01
0·32	0·7912822029	00	−0·55624668	−01	0·60580050	−02	−0·12221	−01
0·35	0·8154917786	00	−0·52467156	−01	0·56200031	−02	−0·10928	−01
0·38	0·8390515708	00	−0·49605168	−01	0·52275156	−02	−0·98137	−02
0·40	0·8544212312	00	−0·47842063	−01	0·49880198	−02	−0·91552	−02
0·42	0·8695365931	00	−0·46183291	−01	0·47643879	−02	−0·85551	−02
0·45	0·8917585916	00	−0·43872015	−01	0·44556751	−02	−0·77506	−02
0·48	0·9134714323	00	−0·41750661	−01	0·41754735	−02	−0·70445	−02
0·495	0·9241472445	00	−0·40754311	−01	0·40449664	−02	−0·67237	−02
0·50	0·9276800398	00	−0·40431112	−01	0·40027883	−02	−0·66210	−02
0·60	0·9958364406	00	−0·34775533	−01	0·32780850	−02	−0·49446	−02
0·70	0·1059807773	01	−0·30336067	−01	0·27292074	−02	−0·37883	−02
0·80	0·1120267657	01	−0·26771959	−01	0·23036177	−02	−0·29632	−02
0·85	0·1149345544	01	−0·25244490	−01	0·21258904	−02	−0·26389	−02
0·90	0·1177727819	01	−0·23857401	−01	0·19671607	−02	−0·23598	−02
0·95	0·1205461255	01	−0·22593160	−01	0·18248449	−02	−0·21184	−02
0·98	0·1221807449	01	−0·21887326	−01	0·17464197	−02	−0·19868	−02
1·00	0·1232587657	01	−0·21436968	−01	0·16967820	−02	−0·19076	−02

Table A.2(a). Wall derivatives of temperature functions in Merk's series, $Pr = 0{\cdot}01$

Λ	$\theta_0'(\Lambda, 0)$		$\theta_1'(\Lambda, 0)$		$\theta_2'(\Lambda, 0)$		$\theta_3'(\Lambda, 0)$	
0·15	0·70805882	−01	0·170736	−02	−0·496979	−03	0·1380	−01
0·10	0·71815184	−01	0·133665	−02	−0·350353	−03	0·4399	−02
0·05	0·72470598	−01	0·114530	−02	−0·281752	−03	0·2254	−02
0·0	0·72957181	−01	0·101621	−02	−0·238810	−03	0·1402	−02
0·05	0·73342859	−01	0·919000	−03	−0·208302	−03	0·9692	−03
0·10	0·73660988	−01	0·841338	−03	−0·185132	−03	0·7167	−03
0·20	0·74163766	−01	0·722336	−03	−0·151449	−03	0·4453	−03
0·25	0·74368440	−01	0·675077	−03	−0·138719	−03	0·3670	−03
0·27	0·74443668	−01	0·657877	−03	−0·134165	−03	0·3419	−03
0·30	0·74550322	−01	0·633651	−03	−0·127843	−03	0·3095	−03
0·32	0·74617660	−01	0·618454	−03	−0·123912	−03	0·2908	−03
0·35	0·74713561	−01	0·596947	−03	−0·118418	−03	0·2663	−03
0·38	0·74803890	−01	0·576839	−03	−0·113348	−03	0·2458	−03
0·40	0·74861286	−01	0·564140	−03	−0·110189	−03	0·2338	−03
0·42	0·74916592	−01	0·551963	−03	−0·107160	−03	0·2231	−03
0·45	0·74995913	−01	0·534604	−03	−0·102918	−03	0·2094	−03
0·48	0·75071211	−01	0·518243	−03	−0·989336	−04	0·1979	−03
0·495	0·75107461	−01	0·510409	−03	−0·970516	−04	0·1930	−03
0·50	0·75119346	−01	0·507847	−03	−0·964352	−04	0·1915	−03
0·60	0·75338460	−01	0·461182	−03	−0·853897	−04	0·172	−03
0·70	0·75527813	−01	0·421812	−03	−0·763634	−04	0·17	−03
0·80	0·75693761	−01	0·388128	−03	−0·788174	−04		
0·85	0·75769438	−01	0·373039	−03	−0·654899	−04		
0·90	0·75840875	−01	0·358964	−03	−0·625142	−04		
0·95	0·75908464	−01	0·345811	−03	−0·596639	−04		
0·98	0·75947315	−01	0·338318	−03	−0·580805	−04		
1·00	0·75972547	−01	0·333483	−03	−0·570806	−04		

Table A.2(b). Wall derivatives of temperature functions in Merk's series, $Pr = 0{\cdot}1$

Λ	$\theta_0'(\Lambda, 0)$		$\theta_1'(\Lambda, 0)$		$\theta_2'(\Lambda, 0)$		$\theta_3'(\Lambda, 0)$	
−0·15	0·18392003	00	0·149640	−02	−0·170851	−02	0·5442	−01
−0·10	0·19043811	00	0·313229	−02	−0·145993	−02	0·1809	−01
−0·05	0·19476614	00	0·355800	−02	−0·129596	−02	0·9630	−02
0·0	0·19803148	00	0·365822	−02	−0·117102	−02	0·6198	−02
0·05	0·20065329	00	0·363428	−02	−0·106993	−02	0·4419	−02
0·10	0·20283959	00	0·355625	−02	−0·985358	−03	0·3355	−02
0·20	0·20634142	00	0·334175	−02	−0·850196	−03	0·2172	−02
0·25	0·20778433	00	0·322681	−02	−0·794968	−03	0·1815	−02
0·27	0·20831732	00	0·318101	−02	−0·774683	−03	0·1698	−02
0·30	0·20907548	00	0·311300	−02	−0·745963	−03	0·1544	−02
0·32	0·20955570	00	0·306830	−02	−0·727862	−03	0·1454	−02
0·35	0·21024171	00	0·300239	−02	−0·702143	−03	0·1333	−02
0·38	0·21089015	00	0·293801	−02	−0·677999	−03	0·1227	−02
0·40	0·21130336	00	0·289600	−02	−0·662706	−03	0·1164	−02
0·42	0·21170240	00	0·285476	−02	−0·648011	−03	0·1106	−02
0·45	0·21227624	00	0·279434	−02	−0·627014	−03	0·1026	−02
0·48	0·21282268	00	0·273568	−02	−0·607179	−03	0·9555	−03
0·495	0·21308633	00	0·270701	−02	−0·597668	−03	0·9229	−03
0·50	0·21317287	00	0·269755	−02	−0·594555	−03	0·9123	−03
0·60	0·21477585	00	0·251839	−02	−0·537728	−03	0·7357	−03
0·70	0·21617330	00	0·235724	−02	−0·489643	−03	0·6064	−03
0·80	0·21740775	00	0·221228	−02	−0·448463	−03	0·5086	−03
0·85	0·21797384	00	0·214528	−02	−0·430026	−03	0·468	−03
0·90	0·21851006	00	0·208163	−02	−0·412654	−03		
0·95	0·21901908	00	0·202111	−02	−0·396677	−03		
0·98	0·21931256	00	0·198622	−02	−0·387825	−03		
1·00	0·21950324	00	0·196353	−02	−0·382714	−03		

Table A.2(c). Wall derivatives of temperature functions in Merk's series, $Pr = 0{\cdot}7$

Λ	$\theta'_0(\Lambda, 0)$		$\theta'_1(\Lambda, 0)$		$\theta'_2(\Lambda, 0)$		$\theta'_3(\Lambda, 0)$	
−0·15	0·36437310	00	−0·143080	−01	−0·220544	−02	0·1213	00
−0·10	0·38697144	00	−0·170425	−02	−0·281147	−02	0·4058	−01
−0·05	0·40223618	00	0·285552	−02	−0·287760	−02	0·2195	−01
0·0	0·41391234	00	0·504331	−02	−0·281456	−02	0·1440	−01
0·05	0·42339971	00	0·621307	−02	−0·271093	−02	0·1047	−01
0·10	0·43139604	00	0·686238	−02	−0·259549	−02	0·8096	−02
0·20	0·44438443	00	0·739469	−02	−0·236714	−02	0·5420	−02
0·25	0·44980780	00	0·746032	−02	−0·226072	−02	0·4599	−02
0·27	0·45182258	00	0·746471	−02	−0·221993	−02	0·4328	−02
0·30	0·45469958	00	0·745368	−02	−0·216069	−02	0·3968	−02
0·32	0·45652881	00	0·743667	−02	−0·212250	−02	0·3756	−02
0·35	0·45915149	00	0·739953	−02	−0·206711	−02	0·3470	−02
0·38	0·46164123	00	0·735117	−02	−0·201396	−02	0·3218	−02
0·40	0·46323332	00	0·731395	−02	−0·197973	−02	0·3067	−02
0·42	0·46477502	00	0·727346	−02	−0·194643	−02	0·2927	−02
0·45	0·46699943	00	0·720770	−02	−0·189817	−02	0·2735	−02
0·48	0·46912590	00	0·713718	−02	−0·185186	−02	0·2563	−02
0·495	0·47015489	00	0·710051	−02	−0·182941	−02	0·2483	−02
0·50	0·47049304	00	0·708811	−02	−0·182203	−02	0·2457	−02
0·60	0·47679616	00	0·682773	−02	−0·168436	−02	0·2021	−02
0·70	0·48235487	00	0·655790	−02	−0·156361	−02	0·1695	−02
0·80	0·48731812	00	0·629120	−02	−0·145713	−02	0·1444	−02
0·85	0·48961155	00	0·616112	−02	−0·140854	−02	0·1339	−02
0·90	0·49179451	00	0·603385	−02	−0·136271	−02	0·1246	−02
0·95	0·49387645	00	0·590969	−02	−0·131944	−02	0·1162	−02
0·98	0·49508063	00	0·583675	−02	−0·129463	−02	0·1116	−02
1·00	0·49586569	00	0·578879	−02	−0·127853	−02	0·1086	−02

Table A.2(d). Wall derivatives of temperature functions in Merk's series, $Pr = 1$

Λ	$\theta'_0(\Lambda, 0)$		$\theta'_1(\Lambda, 0)$		$\theta'_2(\Lambda, 0)$		$\theta'_3(\Lambda, 0)$	
−0·15	0·40933631	00	−0·197681	−01	−0·222206	−02	0·1406	00
−0·10	0·43679753	00	−0·367636	−02	−0·311802	−02	0·4687	−01
−0·05	0·45537196	00	0·220258	−02	−0·326815	−02	0·2534	−01
0·0	0·46959999	00	0·506246	−02	−0·323329	−02	0·1664	−01
0·05	0·48117747	00	0·662242	−02	−0·313613	−02	0·1210	−01
0·10	0·49094928	00	0·751499	−02	−0·301732	−02	0·9369	−02
0·20	0·50685378	00	0·831034	−02	−0·277044	−02	0·6285	−02
0·25	0·51350838	00	0·844630	−02	−0·265257	−02	0·5339	−02
0·27	0·51598281	00	0·847175	−02	−0·260709	−02	0·5026	−02
0·30	0·51951842	00	0·848643	−02	−0·254078	−02	0·4611	−02
0·32	0·52176781	00	0·848322	−02	−0·249787	−02	0·4365	−02
0·35	0·52499488	00	0·846261	−02	−0·243547	−02	0·4035	−02
0·38	0·52806059	00	0·842661	−02	−0·237541	−02	0·3745	−02
0·40	0·53002217	00	0·839567	−02	−0·233664	−02	0·3570	−02
0·42	0·53192256	00	0·836011	−02	−0·229886	−02	0·3408	−02
0·45	0·53466610	00	0·829956	−02	−0·224402	−02	0·3186	−02
0·48	0·53729063	00	0·823203	−02	−0·219128	−02	0·2987	−02
0·495	0·53856128	00	0·819613	−02	−0·216568	−02	0·2895	−02
0·50	0·53897894	00	0·818389	−02	−0·215726	−02	0·2865	−02
0·60	0·54677286	00	0·791870	−02	−0·199976	−02	0·2360	−02
0·70	0·55366082	00	0·763363	−02	−0·186105	−02	0·1982	−02
0·80	0·55982323	00	0·734592	−02	−0·173832	−02	0·1691	−02
0·85	0·56267490	00	0·720407	−02	−0·168218	−02	0·1570	−02
0·90	0·56539171	00	0·706453	−02	−0·162919	−02	0·1461	−02
0·95	0·56798513	00	0·692773	−02	−0·157908	−02	0·1364	−02
0·98	0·56948621	00	0·684710	−02	−0·155032	−02	0·1310	−02
1·00	0·57046525	00	0·679399	−02	−0·153166	−02	0·1276	−02

Table A.2(e). Wall derivatives of temperature functions in Merk's series, $Pr = 5$

Λ	$\theta_0'(\Lambda, 0)$		$\theta_1'(\Lambda, 0)$		$\theta_2'(\Lambda, 0)$		$\theta_3'(\Lambda, 0)$	
−0·15	0·68330186	00	−0·558285	−01	−0·279369	−02	0·2840	00
−0·10	0·74362901	00	−0·159038	−01	−0·546172	−02	0·9337	−01
−0·05	0·78434114	00	−0·138098	−02	−0·605684	−02	0·5020	−01
0·0	0·81556125	00	0·573642	−02	−0·613100	−02	0·3284	−01
0·05	0·84103038	00	0·969494	−02	−0·602159	−02	0·2383	−01
0·10	0·86259826	00	0·120401	−01	−0·584057	−02	0·1842	−01
0·20	0·89789713	00	0·143397	−01	−0·541959	−02	0·1232	−01
0·25	0·91275733	00	0·148541	−01	−0·520945	−02	0·1045	−01
0·27	0·91829892	00	0·149889	−01	−0·512747	−02	0·9830	−02
0·30	0·92623326	00	0·151329	−01	−0·500725	−02	0·9013	−02
0·32	0·93129158	00	0·151964	−01	−0·492908	−02	0·8530	−02
0·35	0·93856327	00	0·152520	−01	−0·481496	−02	0·7881	−02
0·38	0·94548835	00	0·152682	−01	−0·470467	−02	0·7310	−02
0·40	0·94992835	00	0·152610	−01	−0·463328	−02	0·6966	−02
0·42	0·95423682	00	0·152417	−01	−0·456359	−02	0·6648	−02
0·45	0·96046933	00	0·151934	−01	−0·446220	−02	0·6214	−02
0·48	0·96644583	00	0·151259	−01	−0·436451	−02	0·5823	−02
0·495	0·96934449	00	0·150862	−01	−0·431701	−02	0·5643	−02
0·50	0·97029802	00	0·150722	−01	−0·430137	−02	0·5585	−02
0·60	0·98816357	00	0·147289	−01	−0·400827	−02	0·4597	−02
0·70	0·10040734	01	0·143132	−01	−0·374914	−02	0·3861	−02
0·80	0·10184126	01	0·138685	−01	−0·351924	−02	0·3295	−02
0·85	0·10250840	01	0·136431	−01	−0·341391	−02	0·3059	−02
0·90	0·10314621	01	0·134183	−01	−0·331435	−02	0·2848	−02
0·95	0·10375712	01	0·131954	−01	−0·322015	−02	0·2659	−02
0·98	0·10411168	01	0·130630	−01	−0·316602	−02	0·2556	−02
1·00	0·10434331	01	0·129755	−01	−0·313089	−02	0·2488	−02

Table A.2(f). Wall derivatives of temperature functions in Merk's series, $Pr = 10$

Λ	$\theta_0'(\Lambda, 0)$		$\theta_1'(\Lambda, 0)$		$\theta_2'(\Lambda, 0)$		$\theta_3'(\Lambda, 0)$	
−0·15	0·85084868	00	−0·786843	−01	−0·352775	−02	0·3866	00
−0·10	0·93265297	00	−0·228181	−01	−0·724162	−02	0·1265	00
−0·05	0·98764038	00	−0·281195	−02	−0·804489	−02	0·6783	−01
0·0	0·10297473	01	0·689437	−02	−0·813420	−02	0·4427	−01
0·05	0·10640859	01	0·122551	−01	−0·797758	−02	0·3204	−01
0·10	0·10931711	01	0·154154	−01	−0·772764	−02	0·2470	−01
0·20	0·11408161	01	0·185023	−01	−0·715619	−02	0·1645	−01
0·25	0·11608996	01	0·191926	−01	−0·687366	−02	0·1393	−01
0·27	0·11683941	01	0·193739	−01	−0·676379	−02	0·1310	−01
0·30	0·11791300	01	0·195684	−01	−0·660298	−02	0·1199	−01
0·32	0·11859778	01	0·196550	−01	−0·649862	−02	0·1134	−01
0·35	0·11958272	01	0·197320	−01	−0·634650	−02	0·1047	−01
0·38	0·12052130	01	0·197569	−01	−0·619974	−02	0·9704	−02
0·40	0·12112340	01	0·197498	−01	−0·610488	−02	0·9242	−02
0·42	0·12170791	01	0·197266	−01	−0·601237	−02	0·8816	−02
0·45	0·12255390	01	0·196664	−01	−0·587794	−02	0·8233	−02
0·48	0·12336568	01	0·195810	−01	−0·574858	−02	0·7711	−02
0·495	0·12375959	01	0·195304	−01	−0·568574	−02	0·7469	−02
0·50	0·12388920	01	0·195125	−01	−0·566506	−02	0·7391	−02
0·60	0·12632030	01	0·190724	−01	−0·527816	−02	0·6072	−02
0·70	0·12848999	01	0·185377	−01	−0·493716	−02	0·5091	−02
0·80	0·13044968	01	0·179654	−01	−0·463535	−02	0·4339	−02
0·85	0·13136288	01	0·176754	−01	−0·449729	−02	0·4025	−02
0·90	0·13223684	01	0·173862	−01	−0·436692	−02	0·3745	−02
0·95	0·13307482	01	0·170997	−01	−0·424366	−02	0·3495	−02
0·98	0·13356154	01	0·169296	−01	−0·417288	−02	0·3358	−02
1·00	0·13387968	01	0·168170	−01	−0·412696	−02	0·3270	−02

Table A.2(g). Wall derivatives of temperature functions in Merk's series, $Pr = 100$

Λ	$\theta_0'(\Lambda, 0)$		$\theta_1'(\Lambda, 0)$		$\theta_2'(\Lambda, 0)$		$\theta_3'(\Lambda, 0)$	
−0·15	0·17772150	01	−0·210392	00	−0·925267	−02	0·1023	01
−0·10	0·19831270	01	−0·578866	−01	−0·186168	−01	0·3305	00
−0·05	0·21193184	01	−0·671903	−02	−0·202392	−01	0·1757	00
0·0	0·22229058	01	0·170770	−01	−0·201615	−01	0·1137	00
0·05	0·23071280	01	0·297878	−01	−0·195610	−01	0·8157	−01
0·10	0·23783857	01	0·370567	−01	−0·187940	−01	0·6239	−01
0·20	0·24951462	01	0·438377	−01	−0·172051	−01	0·4097	−01
0·25	0·25444333	01	0·452382	−01	−0·164572	−01	0·3448	−01
0·27	0·25628429	01	0·455829	−01	−0·161707	−01	0·3235	−01
0·30	0·25892337	01	0·459258	−01	−0·157549	−01	0·2954	−01
0·32	0·26060803	01	0·460585	−01	−0·154872	−01	0·2788	−01
0·35	0·26303307	01	0·461413	−01	−0·150997	−01	0·2566	−01
0·38	0·26534635	01	0·461106	−01	−0·147285	−01	0·2372	−01
0·40	0·26683160	01	0·460389	−01	−0·144899	−01	0·2255	−01
0·42	0·26827451	01	0·459331	−01	−0·142582	−01	0·2148	−01
0·45	0·27036482	01	0·457208	−01	−0·139230	−01	0·2001	−01
0·48	0·27237280	01	0·454560	−01	−0·136021	−01	0·1870	−01
0·495	0·27334799	01	0·453075	−01	−0·134468	−01	0·1809	−01
0·50	0·27366898	01	0·452559	−01	−0·133957	−01	0·1790	−01
0·60	0·27970169	01	0·440625	−01	−0·124473	−01	0·1461	−01
0·70	0·28510652	01	0·426955	−01	−0·116205	−01	0·1219	−01
0·80	0·29000712	01	0·412755	−01	−0·108952	−01	0·1034	−01
0·85	0·29229740	01	0·405667	−01	−0·105652	−01	0·9577	−02
0·90	0·29449342	01	0·398655	−01	−0·102547	−01	0·8896	−02
0·95	0·29660300	01	0·391751	−01	−0·996184	−02	0·8288	−02
0·98	0·29783015	01	0·387671	−01	−0·979408	−02	0·7954	−02
1·00	0·29863301	01	0·384979	−01	−0·968537	−02	0·7742	−02

Table A.3. Functions related to displacement thickness

Λ	$\delta_{1,s}^*(\Lambda)$	$f_1(\Lambda, \infty)$	$f_2(\Lambda, \infty)$	$f_3(\Lambda, \infty)$
−0·15	1·64697	−1·03100	0·164068	−2·00140
−0·10	1·44270	−0·559175	0·086114	−0·632520
−0·05	1·31236	−0·374228	0·056019	−0·310977
0·0	1·21678	−0·274603	0·040050	−0·183335
0·05	1·14174	−0·212536	0·030250	−0·119524
0·10	1·08032	−0·170425	0·023699	−0·083117
0·20	0·98416	−0·117576	0·015649	−0·045503
0·25	0·94533	−0·100138	0·013054	−0·035145
0·27	0·93111	−0·094253	0·012187	−0·031889
0·30	0·91099	−0·086362	0·011033	−0·027720
0·32	0·89832	−0·081645	0·010348	−0·025335
0·35	0·88030	−0·075264	0·009428	−0·022243
0·38	0·86337	−0·069605	0·008619	−0·019629
0·40	0·85263	−0·066178	0·008133	−0·018107
0·42	0·84229	−0·062997	0·007684	−0·016736
0·45	0·82751	−0·058636	0·007072	−0·014922
0·48	0·81349	−0·054709	0·006526	−0·013357
0·495	0·80676	−0·052889	0·006275	−0·012653
0·50	0·80455	−0·052303	0·006194	−0·012428
0·60	0·76397	−0·042331	0·004839	−0·008851
0·70	0·72910	−0·034916	0·003858	−0·006484
0·80	0·69868	−0·029251	0·003128	−0·004835
0·85	0·68486	−0·026907	0·002832	−0·004210
0·90	0·67183	−0·024826	0·002572	−0·003678
0·95	0·65954	−0·022969	0·002344	−0·003233
0·98	0·65248	−0·021950	0·002219	−0·002929
1·00	0·64790	−0·021306	0·002141	−0·002820

Table A.4. Integrals related to momentum thickness

Λ	$I_0 = \delta^*_{2,s}$	I_1	I_2	I_3
−0·15	0·545184	0·173751	−0·029827	0·238793
−0·10	0·515044	0·129761	−0·021580	0·116992
−0·05	0·490464	0·103525	−0·016755	0·073403
0·0	0·469600	0·085481	−0·013495	0·050972
0·05	0·451469	0·072177	−0·011133	0·037482
0·10	0·435457	0·061939	−0·009345	0·028619
0·20	0·408230	0·047243	−0·006837	0·017979
0·25	0·396485	0·041818	−0·005934	0·014636
0·27	0·392074	0·039909	−0·005619	0·013532
0·30	0·385735	0·037281	−0·005190	0·012076
0·32	0·381681	0·035671	−0·004928	0·011218
0·35	0·375841	0·033443	−0·004569	0·010076
0·38	0·370267	0·031416	−0·004245	0·009081
0·40	0·366690	0·030163	−0·004047	0·008488
0·42	0·363212	0·028368	−0·003860	0·007939
0·45	0·358191	0·027338	−0·003603	0·007209
0·48	0·353373	0·025824	−0·003368	0·006561
0·495	0·351037	0·025113	−0·003258	0·006263
0·50	0·350269	0·024882	−0·003222	0·006167
0·60	0·335906	0·020850	−0·002610	0·004595
0·70	0·323203	0·017701	−0·002145	0·003490
0·80	0·311842	0·015194	−0·001784	0·002668
0·85	0·306601	0·014129	−0·001634	0·002349
0·90	0·301617	0·013167	−0·001500	0·002071
0·95	0·296859	0·012297	−0·001380	0·001838
0·98	0·294120	0·011813	−0·001315	0·001638
1·00	0·292339	0·011506	−0·001273	0·001603

SUR LA METHODE DE MERK POUR LE CALCUL DU TRANSFERT EN COUCHE LIMITE

Résumé—On examine en détail la procédure de Merk pour le calcul du transfert en couche limite à partir des solutions du coin. Sont fausses les équations différentielles gouvernant la fonction universelle dans le second terme de sa solution en développement en série, pour les équations de quantité de mouvement et d'énergie. On a obtenu des solutions numériques des équations corrigées. On a de plus évalué et tabulé les fonctions universelles associées aux deux termes d'ordre supérieur. Avec une telle information, on peut évaluer la précision des résultats. On donne des exemples qui illustrent la commodité aussi bien que les limites de la méthode.

DIE MERK'SCHE BERECHNUNGSMETHODE DES GRENZSCHICHT-ÜBERGANGS

Zusammenfassung—Die Merk'sche Methode zur Berechnung von Grenzschichtübergängen unter Benützung von Keillösungen wird im Einzelnen überprüft. Die Differentialgleichungen, welche die universelle Funktion im 2. Term der Reihenentwicklung für Impuls- und Energiegleichung von Grenzschichten beeinflussen, sind fehlerbehaftet. Numerische Lösungen für die korrekten Gleichungen wurden erhalten. Zusätzlich wurden die mit den zwei Gliedern höherer Ordnung verknüpften universellen Funktionen entwickelt und tabelliert. Damit lässt sich die Genauigkeit der Ergebnisse beurteilen. An Beispielen werden Brauchbarkeit und Grenzen der Methode gezeigt.

О МЕТОДЕ МЕРКА РАСЧЕТА ПЕРЕНОСА В ПОГРАНИЧНОМ СЛОЕ

Аннотация—На примере решений для клина подробно рассматривается метод Мерка расчета переноса в пограничном слое. Дифференциальные уравнения, описывающие универсальную функцию во втором члене предложенного им решения в виде ряда для уравнений пограничного слоя для импульса и энергии, являются ошибочными. Получены численные решения исправленных уравнений. Кроме того, проведен расчет и составлены таблицы универсальных функций для двух членов высшего порядка. При наличии такой информации можно с достоверностью говорить о точности результатов. На примерах показаны достоинства и ограничения, свойственные методу.